International Journal of GEOMATE, Jan., 2021, Vol.20, Issue 77, pp. 107-115
ISSN: 2186-2982 (P), 2186-2990 (O), Japan, DOI: https://doi.org/10.21660/2020.77.28817
Geotechnique, Construction Materials and Environment

EVALUATION OF DYNAMIC INTERACTION FACTOR OF RECTANGULAR PILED RAFT FOUNDATION FOR HORIZONTAL AND ROTATIONAL MOTION

* Hiroshi Nagai[1]

[1] College of Design and Manufacturing Technology, Muroran Institute of Technology, Japan

*Corresponding Author, Received: 13 Sep. 2020, Revised: 24 Nov. 2020, Accepted: 11 Dec. 2020

ABSTRACT: The interaction between a building and the soil its foundation is built into is important in evaluating the seismic response of the building. The dynamic impedance of a piled raft foundation depends on a dynamic interaction factor between the raft and pile group. In this paper, numerical analyses were performed to investigate the frequency characteristics of the dynamic interaction factor of a rectangular piled raft foundation with various aspect ratios, subjected to a building inertial force caused by an earthquake. Based on the analytical results, a formula was proposed that considers the aspect ratio of the foundation in evaluatiing the dynamic interaction factor for a rectangular piled raft foundation. It was confirmed that the dynamic impedance calculated by a simplified calculation using the dynamic interaction factor and the dynamic impedances of a spread foundation and pile foundation, corresponds well with the results of the numerical analysis.

Keywords: Piled raft foundation, Dynamic impedance, Interaction factor, Rectangular, Aspect ratio

1. INTRODUCTION

The piled raft foundation design combines the features of spread and pile foundations, allowing greater optimization of foundations than can be achieved in previous designs. However, the piled raft foundation has the interaction between raft and pile, the evaluation of the seismic response of a building must take into account the dynamic interactions between the building and the soil.

Some shaking table tests on model piled raft foundation have been conducted by several researchers [1, 2]. These studies revealed how the vibration characteristics and the pile stresses of piled raft foundations differ from the those of pile foundations. Recently, the seismic monitoring of the actual building supported by a piled raft foundation has been reported [3, 4]. On the other hand, in seismic response analyses of buildings supported by piled raft foundations, it is important to consider the soil-structure interaction. Finite element method (FEM) has been employed for seismic response analysis considering soil-structure interaction of piled raft foundation [5, 6, 7]. FEM analysis enables detailed calculations to be carried out, but a large-scale 3D analysis requires a huge computational capacity and long calculation times. Thus, it is desirable to establish a convenient evaluation method that can be applied during the design of an actual building.

The sway-rocking model is a simple dynamic analysis method that considers the soil–structure interaction. However, this method requires knowledge of the dynamic impedance that expresses the soil resistance against the horizontal and rotational motions of the foundation. Regarding the dynamic impedances of piled raft foundations, Nakai et al. [8] have reported the effect of the number of piles and the embedment into the soil on the horizontal dynamic impedance, calculated using a finite element method. Emani and Maheshwari [9] have investigated the influences of the pile spacing and the embedment into the soil on the vertical, horizontal, and rotational dynamic impedances using a consistent infinitesimal finite element cell method. Fukuwa and Wen [10] have compared piled raft foundations with spread foundations and pile foundations regarding the horizontal, vertical, and rotational dynamic impedances. In addition, the vertical impedance of piled raft foundations has been studied by other researchers [11, 12]. Although it is possible to obtain the dynamic impedance of piled raft foundations by the above method, detailed calculations are required.

The author [13] has proposed a simplified method for calculating the dynamic impedance of piled raft foundations based on three factors, the dynamic impedance of the spread foundation, the dynamic impedance of the pile foundation, and a dynamic interaction factor between the raft and pile group constituting the piled raft foundation. The dynamic interaction factor, which is a key to the method, is formulated by an arbitrary function based on a numerical analysis varying the conditions of the foundation and soil. However, the shape of the foundation in the analysis has been limited to a square.

For a rectangular pile foundation, Gazetas et al. [14] pointed out that the frequency characteristics of the rotational dynamic impedance strongly depend on the pile configuration. A similar tendency was reported in reference [15]. Therefore, the aspect ratio of the foundation may affect the frequency characteristics of the dynamic interaction factor between the raft and pile group of the piled raft foundation.

The objective of this paper is to evaluate the dynamic interaction factor required to easily calculate the horizontal and rotational dynamic impedance of a rectangular pile raft foundation subjected to inertial loading due to an earthquake. Firstly, parametric numerical analyses were performed on rectangular piled raft foundations with various aspect ratios to investigate the frequency characteristics of the dynamic interaction factor for horizontal and rotational motions. Secondary, based on the analytical results, a new evaluation formula of the dynamic interaction factor was proposed that takes into account the aspect ratio of the foundation. Finally, it was confirmed that the proposed dynamic interaction factor can be applied to the dynamic impedance of piled raft foundations by a simplified calculation.

2. SIMPLIFIED CALCULATION AND NUMERICAL ANALYSIS

2.1 Outline of a Simplified Calculation for the Dynamic Impedance of a Piled Raft Foundation

Clancy and Randolph [16] have proposed the approximate method shown in Eq. (1) to calculate the overall stiffness for static settlement of piled raft foundations. This method is shown in reference [17] as one of the designs of the piled raft foundation.

The simplified calculation was founded by extending its method to a dynamic problem. The dynamic impedance of a foundation subjected to a dynamic load is complex and includes stiffness and damping. In dynamic problems, the values k_{PR}, k_r, k_p, and α_{rp} in Eq. (1) below should be replaced with complex values, and transformed as shown in Eq. (2).

$$\frac{k_{PR}}{k_p} = \frac{1+(1-2\alpha_{rp})(k_r/k_p)}{1-\alpha_{rp}^{\ 2}(k_r/k_p)} \tag{1}$$

where k_r, k_p, and k_{PR} are the overall stiffnesses of the raft in isolation, pile group in isolation, and piled raft foundation, respectively, and α_{rp} is the interaction factor of the raft on the pile group.

$$K_{m,PR}(f) = \frac{K_{m,PG}(f)+\{1-2\alpha_{d,m}(f)\}K_{m,SF}(f)}{1-\alpha_{d,m}^{\ 2}(f)\{K_{m,SF}(f)/K_{m,PG}(f)\}} \tag{2}$$

where K_{SF}, K_{PG}, and K_{PR} are the dynamic impedances of the spread, pile, and piled raft foundation, respectively, α_d is the dynamic interaction factor, f is the frequency, and the subscript m is the index of motion (e.g. horizon, rotation).

The simplified method can calculate the dynamic impedance of a piled raft foundation using the dynamic interaction factor and the dynamic impedances of the spread foundation and the pile group foundation. Hence, a practical calculation method for α_d is required in addition to the conventional calculation of K_{SF} and K_{PG}.

2.2 Calculation of Dynamic Impedance and Dynamic Interaction Factor by Numerical Analysis

Fig. 1 is a schematic diagram of the analytical method. The method combines a finite element method and a thin layer method. The raft and pile are modeled as a plate element and beam element by finite element method, respectively. The stiffness of the raft and the pile head connections are assumed to be infinite in the present study. The soil is treated as an inverse matrix of three-dimensional Green's functions derived from the excitation solution in the thin layer method. A ring excitation solution is used when the vertical axes of the excitation points at which the excitation force acts coincide with the vertical axes of the points at which the vibration occurs. Otherwise, a point excitation solution is used. The stiffness of each component is assumed to be represented by a linear viscoelastic model consisting of a spring and a dashpot mounted in parallel.

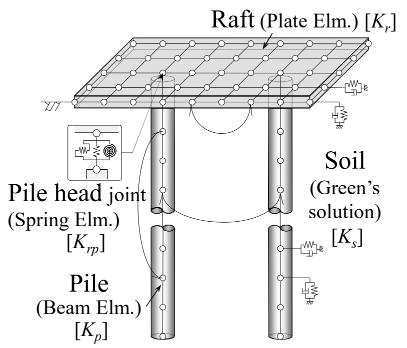

Fig.1 Schematic of analytical method

The dynamic impedance is defined as the ratio of the harmonic load acting on the foundation to the vibration amplitude of the foundation. In this paper, the external force is taken to be the inertial force of a building in response to an earthquake. This force consists of a harmonic horizontal load $Q(f) = Q_0 \cdot \exp(i2\pi ft)$ for horizontal motion and an overturning moment $M(f) = M_0 \cdot \exp(i2\pi ft)$ for rotational motion. The steady-state vibration amplitudes of the horizontal displacement $U(f) = U_0(f) \cdot \exp\{i2\pi ft - i\varphi_{ho}(f)\}$ and the rotational angle of foundation $\theta(f) = \theta_0(f) \cdot \exp\{i2\pi ft - i\varphi_{ro}(f)\}$ under the harmonic load can be calculated by a frequency response analysis of the equation of motion for the foundation–soil system (Eq. (3)).

$$([K^*] - \omega^2 [M]) \cdot \{U(\omega)\} = \{F(\omega)\} \quad (3)$$

where $\{F\}$ is the external force vector acting on the foundation, $\{U\}$ is the displacement vector of the foundation, $[K^*]$ and $[M]$ are, respectively, the complex stiffness matrix and the mass matrix of foundation and soil, and ω is the circular frequency ($= 2\pi f$).

The horizontal and rotational dynamic impedance in the frequency domain (K_{ho}, K_{ro}) are, respectively, expressed by Eqs. (4) and (5).

$$K_{ho}(f) = \frac{Q(f)}{U(f)} = \left| \frac{Q_0}{U_0(f)} \right| \cdot \exp\{i\varphi_{ho}(f)\} \quad (4)$$

$$K_{ro}(f) = \frac{M(f)}{\theta(f)} = \left| \frac{M_0}{\theta_0(f)} \right| \cdot \exp\{i\varphi_{ro}(f)\} \quad (5)$$

where Q_0 and M_0 are, respectively, the amplitudes of the horizontal inertial force and the overturning moment, U_0 is the amplitude of the dynamic horizontal displacement at the foundation, θ_0 is the amplitude of the dynamic rotational angle of the foundation, φ_{ho} is the initial phase angle of the dynamic horizontal displacement, φ_{ro} is the initial phase angle of the dynamic rotational angle, and i is the imaginary unit ($i^2 = -1$).

The dynamic interaction factor α_d can be obtained by substituting the dynamic impedances of the three foundations calculated by numerical analysis (K_{SF}, K_{PG} and K_{PR}) into Eq. (6) which is a modification of Eq. (2), and solving.

$$\left(\frac{K_{m,PR}}{K_{m,PG}} \right) \alpha_{d,m}{}^2 - 2\alpha_{d,m} + \left(\frac{K_{m,PG}}{K_{m,SF}} - \frac{K_{m,PR}}{K_{m,SF}} + 1 \right) = 0 \quad (6)$$

2.3 Analytical Model

Fig. 2 shows the analytical model used in this paper. A semi-infinite soil is assumed, and the foundation slab is considered to be a massless rigid body, and is not embedded into the soil. The piles are cast-in-place concrete piles with diameters of d = 1 m. Eight different cases for the piled raft foundation are considered, with the aspect ratio of the foundation AR ($=B_x/B_y$) varied from 0.17 to 6.00 (Fig. 3, Table 1). For each case, the conditions of the foundation and soil are set up in six patterns with pile spacing s/d, pile length L/d, and soil shear wave velocity V_s, as shown in Table 2. The model in Pattern 1 (s/d = 5, L/d = 25, Vs = 200 m/s) is called the basic model.

A frequency response analysis was performed in the range of 1 to 40 Hz in increments of 1 Hz.

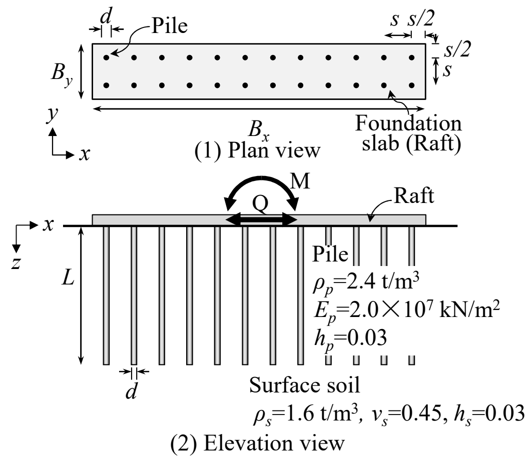

Fig.2 Analytical model

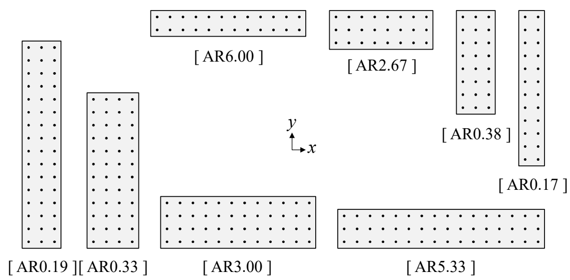

Fig.3 Pile layouts

Table 1 Aspect ratio of rectangular foundation

Case	n	AR	$B_x : B_y$
1	24	0.17	10:60
2	24	0.38	15:40
3	24	2.67	40:15
4	24	6.00	60:10
5	48	0.19	15:80
6	48	0.33	20:60
7	48	3.00	60:20
8	48	5.33	80:15

Table 2 Analysis parameters

Pattern	s/d	L/d	V_s (E_p/E_s)
1	5	25	200 (1.10×10^2)
2	7.5	25	200 (1.10×10^2)
3	10	25	200 (1.10×10^2)
4	5	12.5	200 (1.10×10^2)
5	5	37.5	200 (1.10×10^2)
6	5	25	100 (4.40×10^2)

3. RESULTS AND DISCUSSIONS

3.1 Frequency Characteristics of Dynamic Interaction Factor

Figs. 4 and 5 show the frequency characteristic of the dynamic interaction factor α_d (= $|\alpha|\cdot\exp(i\varphi_\alpha)$; here, $|\alpha|$ is amplitude, and φ_α is initial phase angle.) of the horizontal and rotational motions, respectively. The results of the pattern 1 for the eight cases with different aspect ratios of the foundation are shown. The horizontal axis in the graph represents the frequency a (=$f\cdot s/V_s$), which is made dimensionless using the pile spacing and soil shear wave velocity.

The amplitude $|\alpha|$ reaches a peak at some frequency and then gradually decreases. The initial phase angle φ_α increases with increasing frequency, then passes an inflection point ($\varphi_\alpha = -\pi/2$) and converges to a certain value. This trend reflects the fact that the displacement of the raft itself due to the excitation force and the displacement due to the waves propagating through the ground from the pile to the raft have opposite phases when the frequency exceeds a certain value. Focusing on the effect of the aspect ratio, in the horizontal component, the peak frequency and the inflection point are almost the same regardless of the aspect ratio. In contrast, in the rotational component, the inflection points tend to be almost the same only for similar values of AR. However, the trend of the rotational component for AR = 0.17 is exceptionally different from the result for AR = 0.19. It has been pointed out that the influence of rotational dynamic impedance is significant for a pile foundation in which two rows of piles are arranged in the vibration direction. As the number of piles arranged orthogonal to the vibration increases, the stiffness (real part) decreases and the damping (imaginary part) increases [14]. For AR = 0.17, the phase of the rotational excitation force differs by $\pi/2$ on the left and right of the foundation, so it is considered that the wave propagation from the adjacent piles was easily canceled.

3.2 Practical Formula for Evaluating Dynamic Interaction Factor

The dynamic interaction factor is a complex number that includes the amplitude and initial phase angle. In previous research on square foundations [13], the amplitude and initial phase angle were respectively expressed by Eqs. (7) and (8). It was previously proposed that the coefficient in the equation should be calculated in relation to the foundation width and the static stiffness of the spread foundation and pile foundation. Therefore, the calculation formulas for the coefficients a_i, ξ, and η were investigated based on the analysis results of the rectangular foundation. The value of ζ is a constant and δ has little effect on the result, so no correction was made for these coefficients.

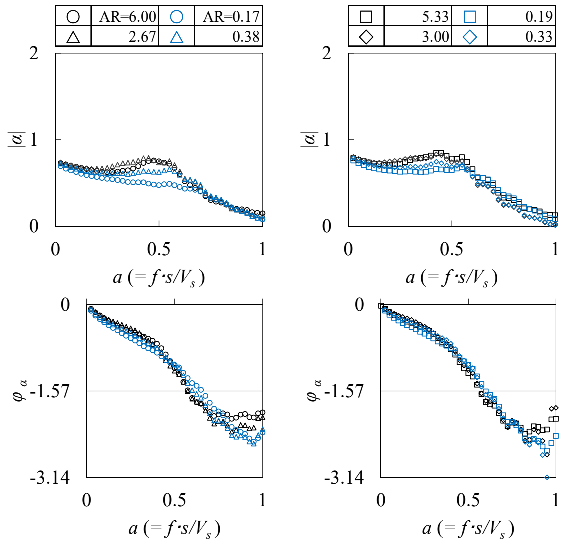

Fig.4 Variation of dynamic interaction factor for horizontal motion

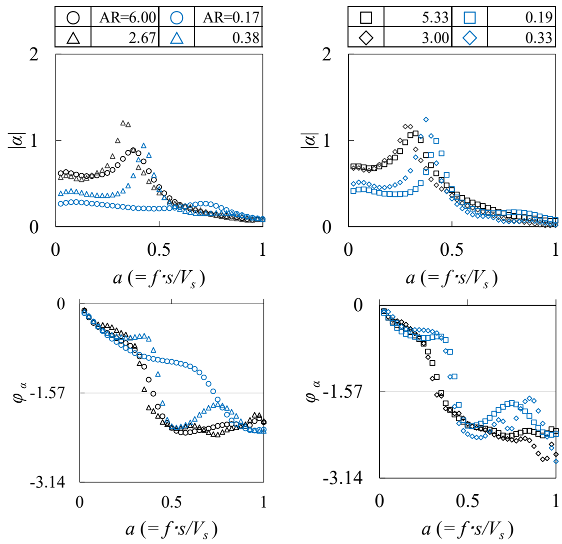

Fig.5 Variation of dynamic interaction factor for rotational motion

$$|\alpha_m(a)| = \frac{\xi\cdot a_i^2}{\sqrt{(\eta\cdot a_i\cdot a)^2 + (a_i^2 - a^2)^2}}\cdot\exp(-\zeta\cdot a) \tag{7}$$

$$\varphi_{\alpha,m}(a) = -\tan^{-1}\left(\frac{\eta\cdot a_i\cdot a+\delta}{a_i^2 - a^2}\right) \tag{8}$$

Fig. 6 shows the relationship between the foundation width B_x and a_i. The coefficient a_i has a value when $\varphi_\alpha = -\pi/2$. The value of the horizontal component shown in Fig. 6(1) generally corresponds with the analytical result and the previous calculation formula for a_i, except for AR = 0.17. On the other hand, the value of the rotation component shown in Fig. 6(2) is often larger than that for the previous calculation formula. It decreases as the foundation width increases, but the trend differs depending on the value of AR. Since a_i is greatly affected by the interaction between adjacent piles [13], B_x is replaced with the width B_x' (effective foundation width; = B_x−s) between the piles located at the outermost circumference in the vibration direction shown in Fig. 7. The relationship between B_x' and a_i is approximated by a power function (Eq. (9)). Fig. 8 shows the relationship between AR and the exponent χ of the power function. Except for AR = 0.17, χ is almost constant for AR ≤ 1.0, and gradually decreases with increasing AR for AR ≥ 1.0. Therefore, the coefficient a_i is defined by the following equations with AR, Eqs. (9)–(11). As an example of the correspondence between B_x' and a_i, the curves for AR = 6.00 and 2.67 were added in Fig. 9.

$$a_i = 1/(B_x')^{\chi} \tag{9}$$

$$AR \leqq 1;\ \chi = 0.333 \tag{10}$$

$$AR > 1;\ \chi = 0.333 \times (AR)^{-0.187} \tag{11}$$

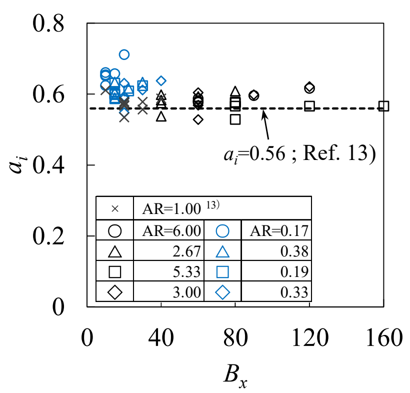

(1) Horizontal

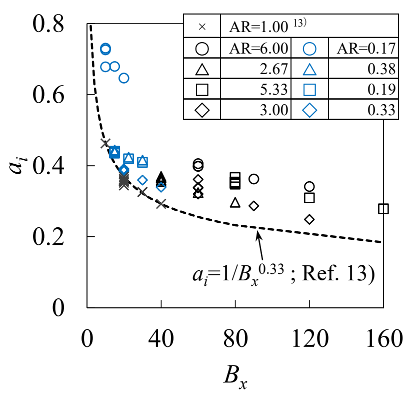

(2) Rotational

Fig.6 Correlation between the width of foundation B_x and the coefficient a_i

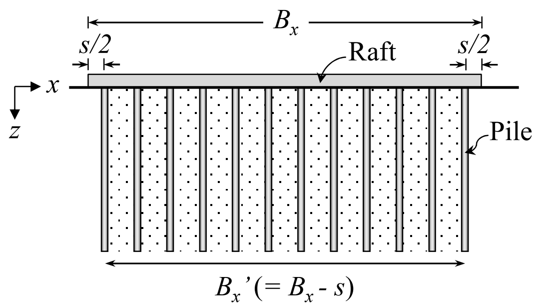

Fig.7 Effective width of foundation

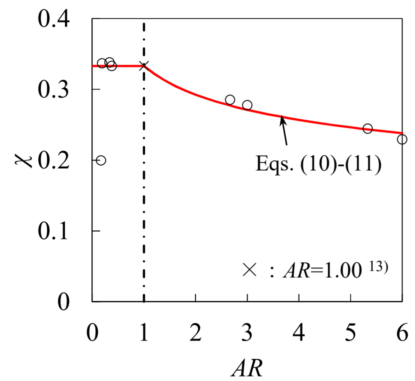

Fig.8 Correlation between the aspect ratio of foundation AR and the exponent χ

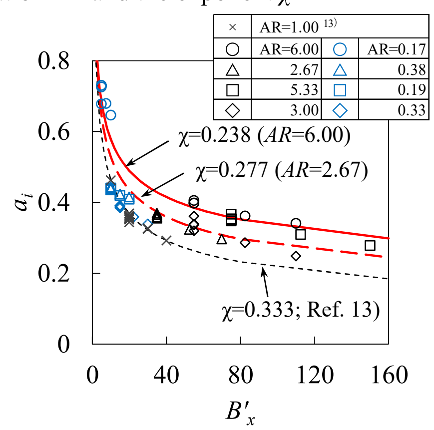

Fig.9 Correlation between the effective width of foundation B_x' and the coefficient a_i

Fig. 10 shows the relationship between $|K_{m,PG}|/|K_{m,SF}|$ and $|K_{m,PR}|/|K_{m,SF}|$. Here, $|K_{m,SF}|$, $|K_{m,PG}|$, and $|K_{m,PR}|$ are the stiffnesses of the foundation calculated at a frequency f = 0.1 Hz, which is close to the static state. The horizontal component shown in Fig. 10(1) almost agrees with the previous calculation formula, but the rotational component shown in Fig. 10(2) has some variation in the relationship due to the aspect ratio. Therefore, the relationship for the rotation component was approximated by Eq. (12), and the relationship between AR and the exponent υ was determined. As shown in Fig. 11, the exponent υ tends to gradually increase as AR increases, and was approximated by

Eq. (13). The coefficient ξ is the value of $|\alpha_m|$ at a = 0, and can be calculated by substituting the three values of $|K_{PG}|$, $|K_{SF}|$, and $|K_{PR}|$ obtained from Eq. (12) into Eq. (6).

$$\left(\left|\frac{K_{ro,PR}}{K_{ro,SF}}\right|\right)^{\upsilon}=\left(\left|\frac{K_{ro,PG}}{K_{ro,SF}}\right|\right)^{\upsilon}+1 \quad (12)$$

$$\upsilon = 2.35\times(AR)^{0.169} \quad (13)$$

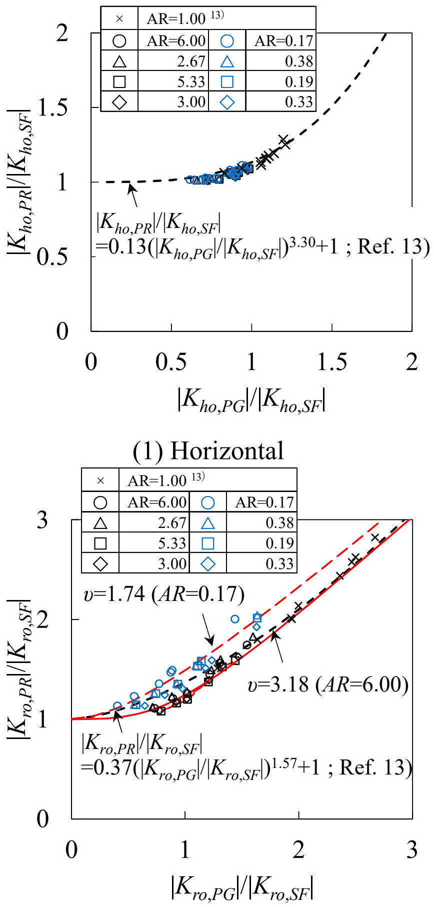

(1) Horizontal

(2) Rotational

Fig.10 Correlation between the stiffness ratio $|K_{m,PG}|/|K_{m,SF}|$ of the pile foundation to the spread foundation and that $|K_{m,PR}|/|K_{m,SF}|$ of the piled raft foundation to the spread foundation

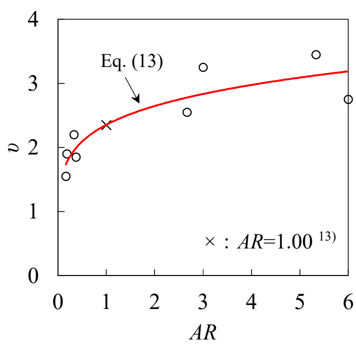

Fig.11 Correlation between the aspect ratio of foundation AR and the exponent υ

Fig. 12 shows the relationship between $|K_{m,PG}|/|K_{m,SF}|$ and η (= $|\alpha_m(0)\cdot\exp(-\xi\cdot a_i)/|\alpha_m(a_i)|$). $|K_{m,SF}|$ and $|K_{m,PG}|$ are the stiffnesses of the foundation calculated at a frequency f = 0.1 Hz. The horizontal component shown in Fig. 12(1) almost agrees with the previous calculation formula. On the other hand, the rotation component shown in Fig. 12(2) shows large variations. This is because the calculation formula for ξ (Eqs. 12 and 13) differs depending on AR for a rectangular foundation. Therefore, the relationship between η/ξ and $|K_{m,PG}|/|K_{m,SF}|$ was investigated. Since the same relationship (Fig. 13) was obtained regardless of the horizontal and rotational components, it was approximated by the following equation, Eq. (14).

$$\frac{\eta}{\xi}=\frac{1}{A'\left(\left|\frac{K_{m,PG}}{K_{m,SF}}\right|\right)^{2}+B'\left(\left|\frac{K_{m,PG}}{K_{m,SF}}\right|\right)+C'} \quad (14)$$

where $A' = -0.235$, $B' = 2.05$, $C' = -0.765$

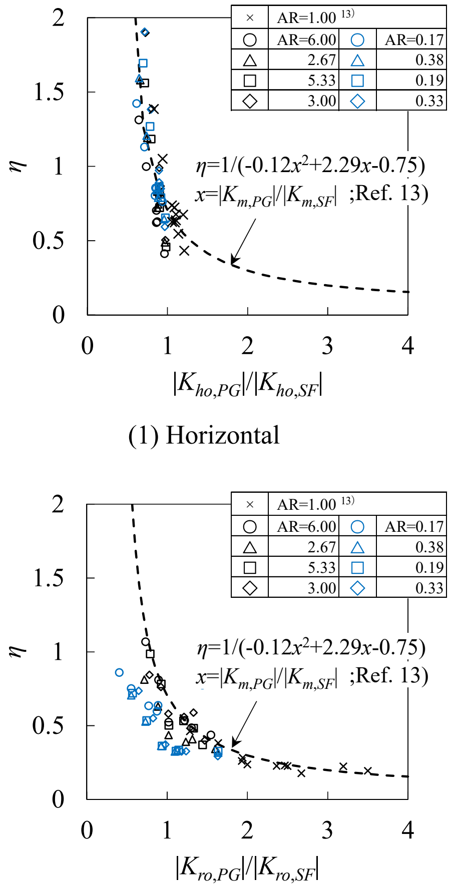

(1) Horizontal

(2) Rotational

Fig.12 Correlation between the stiffness ratio $|K_{m,PG}|/|K_{m,SF}|$ of the pile foundation to the spread foundation and the coefficient η

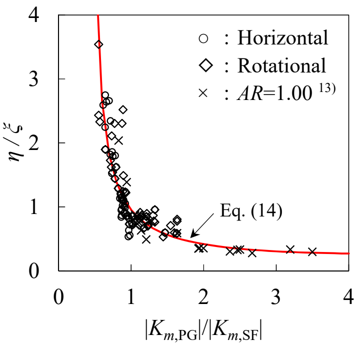

Fig.13 Correlation between the stiffness ratio $|K_{m,PG}|/|K_{m,SF}|$ of the pile foundation to the spread foundation and the coefficient η/ξ

3.3 Comparison between Simplified Calculation and Numerical Analysis for Dynamic Impedance

The applicability of the simplified calculation for the dynamic impedance of the piled raft foundation is verified by a comparison with the results of a numerical analysis method (called Ana). The simplified calculation was performed using the proposed dynamic interaction factor, and the dynamic impedances of the spread foundation and the pile foundation (K_{SF}, K_{PG}) were calculated in two ways, as follows.

The first method (called Cal-1) uses the dynamic ground compliance (DGC) [18] for K_{SF}, and a beam spring model considered a propagation wave between adjacent piles [19, 20, 21] for K_{PG}. The second method (called Cal-2) uses a numerical analysis to calculate K_{SF} and K_{PG}, allowing the effect of α_d in the simplified calculation to be investigated.

The model used for the verification had the same conditions as in the previous section (see Tables 1 and 2), and a maximum frequency set to 9 to 26 Hz. This frequency is considered the applicable range for the DGC, and corresponds to a dimensionless frequency of $\omega\cdot(B_x\times B_y)^{0.5}/2V_s = 10$.

A comparison of the dynamic impedance K_{PR} ($|K|$: amplitude, φ: initial phase angle) using the simplified calculation and the numerical analysis method is displayed in Fig. 14, showing the impedance for the pattern 1 with $AR = 5.33$ and 0.19 ($s/d = 5$, $L/d = 25$, $V_s = 200$ m/s). Cal-2 agrees very well with Ana regardless of AR and the excitations. On the other hand, for Cal-1, the value of $|K|$ is slightly smaller than the Ana result, and the value of φ tends to be slightly larger. These trends were similar for other values of AR.

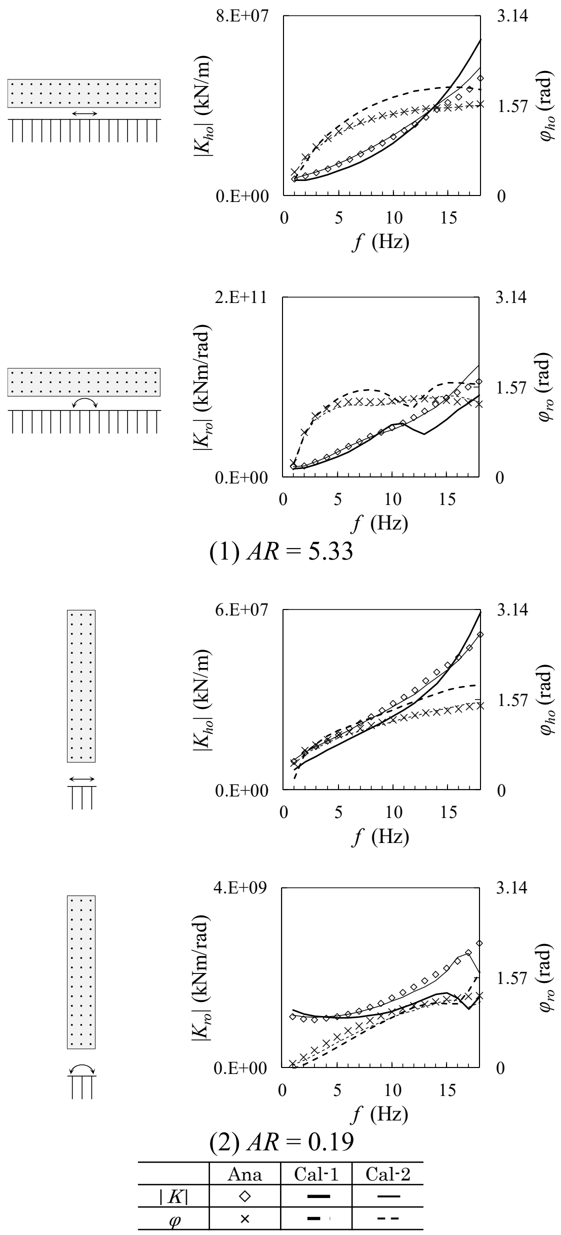

Fig.14 Impedance of piled raft foundation (Pattern 1; $s/d = 5$, $L/d = 25$, $Vs = 200$ m/s)

Fig. 15 shows a comparison of the dynamic impedances for all 48 models (8 cases × 6 patterns). Although Cal-2 exhibits a slight variation in the initial phase angle of the rotation component, it almost corresponds to Ana in the other cases, and the evaluation formula of the dynamic interaction factor is sufficiently accurate regardless of AR. On the other hand, Cal-1 exhibits a large difference from Ana in both the horizontal impedance and rotational impedance. This is because as the frequency increases, different values of K_{SF} and K_{PG} between Ana and Cal-1 are obtained. Therefore, it is important to be aware of this when applying the simplified calculation method.

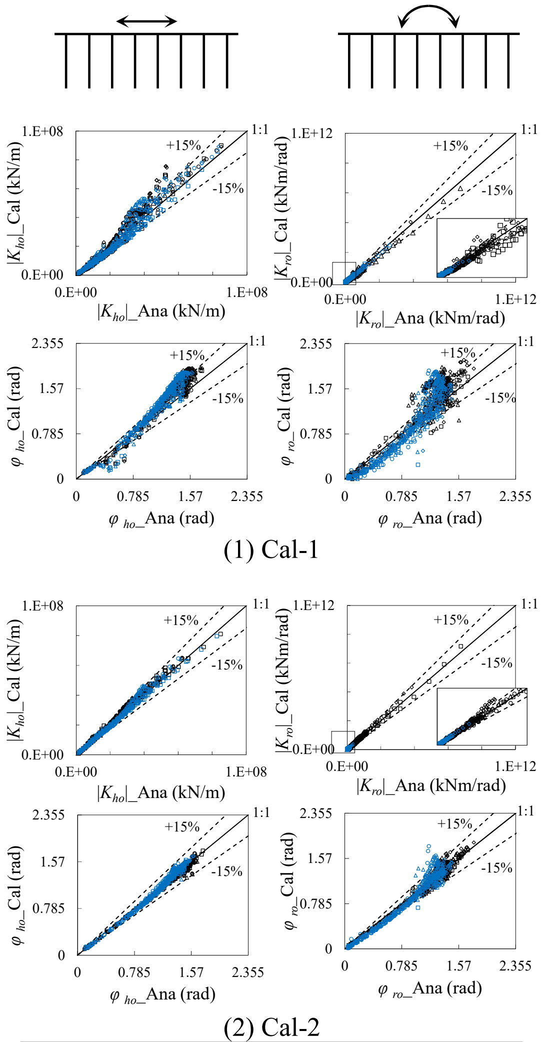

○	AR=6.00	△	2.67	□	5.33	◇	3.00
○	0.17	△	0.38	□	0.19	◇	0.33

Fig.15 Comparison of dynamic impedances obtained using the simplified method and the analytical method

4. CONCLUSIONS

This paper evaluated the dynamic interaction factor required to easily calculate the horizontal and rotational dynamic impedance of the rectangular pile raft foundation subjected to inertial loading due to an earthquake. From the results obtained by numerical analyses that combines the finite element method and the thin layer method, it was revealed that the frequency characteristics of the dynamic interaction factor for rotational motion strongly depend on the aspect ratio of foundation. In contrast, the dynamic interaction factor for horizontal motion remained almost unchanged, even when the aspect ratio of the foundation is increased to 6.

Hence, the author proposed a new formula to evaluate the dynamic interaction factor for the rotation motion of a rectangular foundation by considering the aspect ratio of the foundation. The coefficients (ξ, η, a_i) used to evaluate the dynamic interaction could have determined using the effective width of the foundation and the stiffness ratio of the spread and pile foundations.

It was confirmed that the dynamic impedance obtained by this simplified calculation using the proposed dynamic interaction factor agrees well with the results from numerical analysis.

5. REFERENCES

[1] Horikoshi K., Matsumoto T., Hashizume Y., Watanabe T., Performance of piled raft foundations subjected to dynamic loading. International Journal of Physical Modeling in Geotechnics, Vol.3, Issue 2, 2003, pp.51-62.
[2] Matsumoto T., Fukumura K., Horikoshi K., Oki A., Shaking table tests on model piled rafts in sand considering influence of superstructures. International Journal of Physical Modeling in Geotechnics, Vol.4, Issue 3, 2004, pp.21-38.
[3] Yamashita K., Hamada J., Onimaru S., Higashino M., Seismic behavior of piled raft with ground improvement supporting a base-isolated building on soft ground in Tokyo. Soils and Foundations, Vol.52, Issue 5, 2012, pp.1000-1015.
[4] Yamashita K., Hamada J., Tanikawa T., Static and seismic performance of a friction piled raft combined with grid-form deep mixing walls in soft ground. Soils and Foundations, Vol.56, Issue 3, 2016, pp.559-573.
[5] Eslami M.M., Aminikhah A., Ahmadi M.M., A comparative study on pile group and piled raft foundations (PRF) behavior under seismic loading. Computational Methods in Civil Engineering, Vol. 2, Issue 2, 2011, pp.185-199.
[6] Kumar A., Choudhury D., Katzenbach R., Effect of earthquake on combined piled-raft foundation. International Journal of Geomechanics, Vol.16, Issue 5, 2016, 04016013-1 - 04016013-16.
[7] Yamashita K., Shigeno Y., Hamada J., Der-Wen Chang, Seismic response analysis of piled raft with grid-form deep mixing walls under strong earthquakes with performance-based design concerns. Soils and Foundations, Vol.58, Issue 1, 2018, pp.65-84.
[8] Nakai S., Mano H., Matsuda T., An analysis for stress distribution of piled raft foundations under seismic loading. Proceedings 2nd US-

Japan Workshop on Soil-Structure Interaction, Tsukuba, Japan, 2001, 1-9.

[9] Emani P.K., Maheshwari B.K., Dynamic impedances of pile groups with embedded caps in homogeneous elastic soils using CIFECM. Soil Dynamics and Earthquake Engineering, Vol. 29, Issues 6, 2009, pp.963-973.

[10] Fukuwa N., Wen X., Efficient soil-structure interaction analysis method of a large-scale pile group. 4th US-Japan Workshop on Soil-Structure Interaction, Tsukuba, 2007, 1-13.

[11] Nguyen V.T., Hassen G., Buhan P., Assessing the dynamic stiffness of piled-raft foundations by means of a multiphase model. Computers and Geotechnics, Vol. 71, 2016, pp.124-135.

[12] Liu C.L., Ai Z.Y., Vertical harmonic vibration of piled raft foundations in layered soils. International journal for Numerical and Analytical Methods in Geomechanics, Vol. 41, Issue 17, 2017, pp.1711-1723.

[13] Nagai H., Simplified method of estimating the dynamic impedance of a piled raft foundation subjected to inertial loading due to an earthquake. Computers and Geotechnics, Vol. 105, 2019, pp.69-78.

[14] Gazetas G., Fan K., Kaynia A., Dynamic response of pile groups with different configurations. Soil Dynamic and Earthquake Engineering, Vol. 12, Issue 4, 1993, pp.239-257.

[15] Choudhary S.S., Biswas S., Manna B., Dynamic coupled response of 6-pile groups with different pile arrangements. Japanese Geotechnical Society Special Publication, Vol. 2, Issue 38, 2015, pp.1389-1392.

[16] Clancy P., Randolph M.F., An approximate analysis procedure for piled raft foundations. International Journal for Numerical and Analytical Methods in Geomechanics, Vol. 17, 1993, pp.849-869.

[17] Architectural Institute of Japan, Recommendations for design of building foundations, 2019, pp.297-307. (in Japanese)

[18] Architectural Institute of Japan, Seismic response analysis and design of buildings considering dynamic soil-structure interaction, 2006, pp.327-332. (in Japanese)

[19] Mylonakis G., Gazetas G., Lateral vibration and internal forces of grouped piles in layered soil. Journal of Geotechnical and Geoenvironmental Engineering, Vol. 125, No, 1, 1999, pp.16-25.

[20] Mylonakis G., Gazetas G., Vertical vibration and additional distress of grouped piles in layered soil. Soils and Foundations, Vol. 38, No. 1, 1998, pp.1-14.

[21] Takewaki I., Kishida A., Efficient analysis of pie-group effect on seismic stiffness and strength design of buildings. Soil Dynamic and Earthquake Engineering, 25, 2005, pp.355-367.